Inorg. Chem. **2004**, *43*, 1220–1228

Calix[4]pyrrole Schiff Base Macrocycles. Novel Binucleating Ligands for μ-Oxo Iron Complexes

Jacqueline M. Veauthier, Won-Seob Cho, Vincent M. Lynch, and Jonathan L. Sessler*

Department of Chemistry and Biochemistry, 1 University Station—A5300, The University of Texas at Austin, Austin, Texas 78712-0165

Received October 17, 2003

New bimetallic μ-oxo diferric complexes of several previously reported calix[4]pyrrole Schiff base macrocycles are described. The synthesis of a new member of this class of macrocycles is also reported; it was prepared via an acid-catalyzed condensation between 1,9-bisformyl-5,5-dipropyldipyrromethane and *o*-phenylenediamine. Reactions of the free base macrocycles or their bis-HCl salts with Fe(II) mesitylene, followed by air oxidation, gave the binuclear μ-oxo bis-Fe(III) compounds **6**–**10** in moderate yield. X-ray crystallography data reveal two different coordination environments for the Fe–O–Fe subunit in **6**–**10** that it is suggested can be controlled by altering the reaction conditions. Structural properties of these metalated pyrrolic macrocycles are also compared to those of μ-oxo diferric porphyrins and μ-oxo diferric texaphyrin. Complexes **6**–**10** exhibit two distinct types of M–N bonds that are similar in length to the bonds observed in metallotexaphyrin complexes. However, the electronics of the present systems are very different from those of texaphyrins and porphyrins in that no delocalized bonding patterns are observed within the ligands as a whole.

Introduction

The active sites of many biologically important enzymes contain two or more transition metal centers. The presence of multinuclear metal centers has long been invoked to explain the function of these biologically important species, and to date considerable effort has been devoted to the synthesis of models to increase this understanding. However, for the most part these efforts have relied on the use of multiple ligands rather than single multifunctional macrocycles. The advantage of using a single ligand is that it could stabilize a particular configuration around the metal centers and, hence, support the formation of new structural motifs. Doing so would be particularly interesting in the case of pyrrolic ligands since, without exception, such ligands are used to coordinate single metal centers in nature (e.g. chlorophyll, porphyrin, F430, coenzyme B_{12}, etc.).[1,2] To date there have been a number of synthetic pyrrolic macrocyclic systems that have been shown to stabilize binuclear metal complexes. These ligands include Bowman-James's accordion porphyrins,[3–5] our amethyrins,[6–9] Furuta's N-confused hexaphyrin,[10] Torres's expanded phthalocyanines,[11] and selected oligopyrrolic systems.[12–20] However, to the best of our knowledge, none have been used to prepare a bis-Fe

* Author to whom correspondence should be sent. E-mail: sessler@mail.utexas.edu.

(1) Dolphin, D., Ed. *The Porphyrins*; Academic Press: New York, 1978.
(2) Kadish, K. M., Smith, K. M., Guilard, R., Eds. *The Porphyrin Handbook*; Academic Press: San Diego, 2000.
(3) Acholla, F. V.; Takusgawa, F.; Mertes, K. B. *J. Am. Chem. Soc.* **1985**, *107*, 6902−6908.
(4) Reiter, W. A.; Gerges, A.; Lee, S.; Deffo, T.; Clifford, T.; Danby, A.; Bowman-James, K. *Coord. Chem. Rev.* **1998**, *174*, 343−359.
(5) Gerasimchuk, N. N.; Gerges, A.; Clifford, T.; Danby, A.; Bowman-James, K. *Inorg. Chem.* **1999**, *38*, 5633−5636.
(6) Hannah, S.; Seidel, D.; Sessler, J. L.; Lynch, V. M. *Inorg. Chim. Acta* **2001**, *317*, 211−217.
(7) Sessler, J. L.; Weghorn, S. J.; Hiseada, Y.; Lynch, V. M. *Chem. Eur. J.* **1995**, *1*, 56−67.
(8) Sessler, J. L.; Gebauer, A.; Guba, A.; Scherer, M.; Lynch, V. M. *Inorg. Chem.* **1998**, *37*, 2073−2076.
(9) Weghorn, S. J.; Sessler, J. L.; Lynch, V. M.; Baumann, T. F.; Sibert, J. W. *Inorg. Chem.* **1996**, *35*, 1089−1090.
(10) Srinivasan, A.; Ishizuka, T.; Osuka, A.; Furuta, H. *J. Am. Chem. Soc.* **2003**, *125*, 878−879.
(11) Rodríguez-Morgade, M. S.; Cabezón, B.; Esperanza, S.; Torres, T. *Chem. Eur. J.* **2001**, *7*, 2407−2413.
(12) Narayanan, S. J.; Sridevi, B.; Chandrashekar, T.; Englich, U.; Ruhland-Senge, K. *Inorg. Chem.* **2001**, *40*, 1637−1645.
(13) Wytko, J. A.; Michels, M.; Zander, L.; Lex, J.; Schmickler, H.; Vogel, E. *J. Org. Chem.* **2000**, *65*, 8709−8714.
(14) Bley-Escrich, J.; Gisselbrecht, J.-P.; Vogel, E.; Gross, M. *Eur. J. Inorg. Chem.* **2002**, 2829−2837.
(15) Franceschi, F.; Guillemot, G.; Solari, E.; Floriani, C.; Re, N.; Birkedal, H.; Pattison, P. *Chem. Eur. J.* **2001**, *7*, 1468−1478.
(16) Xie, L. Y.; Dolphin, D. *J. Chem. Soc., Chem. Commun.* **1994**, 1475−1476.
(17) Charriere, R.; Jenny, T.; Rexhausen, H.; Gossauer, A. *Heterocycles* **1993**, *36*, 1561−1575.

10.1021/ic0352001 CCC: $27.50
Published on Web 01/30/2004

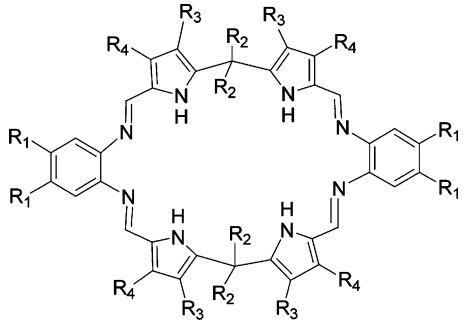

1 R_1 = H, R_2 = CH_3, R_3 = H, R_4 = H
2 R_1 = OCH_3, R_2 = CH_3, R_3 = H, R_4 = H
3 R_1 = H, R_2 = H, R_3 = CH_2CH_3, R_4=CH_3
4 R_1 = H, R_2 = $CH_2CH_2CH_3$, R_3= H, R_4 = H

Figure 1. Calix[4]pyrrole Schiff base macrocycles.

species containing a pyrrolic μ-oxo M−O−M bridge stabilized by one macrocyclic ligand.

We recently reported the synthesis, characterization, and anion binding properties of three new octa-aza calix[4]pyrrole Schiff base macrocycles **1**−**3** (Figure 1).[21] These new macrocycles have large binding cavities that, on the basis of modeling studies, appear big enough to accommodate at least two metal centers. This has prompted us to consider their use as cation coordinating ligands. As a first test of this premise, we have carried out studies using Fe(III) as the targeted transition metal center and wish to report here the synthesis and characterization of the μ-oxo diferric compounds of **1**−**3**. We also report the synthesis of a new dipropyl calix[4]pyrrole Schiff base macrocycle, **4**, and its Fe(III) coordinated complex.

Experimental Section

General Procedures. All reactions and manipulations were carried out under an atmosphere of dry, oxygen-free argon by means of standard Schlenk techniques or a Vacuum Atmospheres drybox unless otherwise stated. Prior to use, all glassware were soaked in KOH-saturated isopropyl alcohol for ca. 12 h and then rinsed with water and acetone before being thoroughly dried. Air sensitive filtrations were performed using positive argon pressure to force solutions through a specially constructed filtration cannula. This was made by fitting the port end of a stainless steel cannula with a piece of hardened filter paper (Whatman's No. 5) and then securing it with Teflon tape. The port of the cannula was made by welding a stainless steel filter support to one end of the cannula purchased from Popper & Sons Inc. Solutions were stirred magnetically. Bath temperatures of −78 °C were maintained with dry ice and acetone.

Tetrahydrofuran (THF), diethyl ether (Et_2O), methanol, toluene, and *N*,*N*-dimethylformamide (DMF) were dried by passage through two columns of activated alumina. Dichloromethane was freshly distilled from calcium hydride. *n*-Pentane was stirred over concentrated H_2SO_4 for more than 24 h, neutralized with K_2CO_3, and distilled from CaH_2. Hexanes were purchased from Fisher Scientific and used as received. All deuterated NMR solvents were purchased from Cambridge Isotope Labs and used as received.

Unless otherwise stated, all reagents were used as received. Triethylamine (Et_3N) was purchased from Acros Organics. *o*-Phenylenediamine and $POCl_3$ were purchased from Aldrich Chemical Co. Iron(II) mesitylene (Fe_2Mes_4)[22−24] and Schiff base macrocycles **1**−**3**[21] were prepared according to previously published procedures.

Nuclear magnetic resonance (NMR) spectra were obtained on a Varian Mercury 400 MHz, a Varian Unity 300 MHz, or a Brüker AC 250 MHz spectrometer. Low- and high-resolution mass spectra were obtained at the University of Texas at Austin Department of Chemistry and Biochemistry MS Facility. Elemental analyses were performed by Atlantic Microlabs Inc., Norcross, GA.

Preparation of 1,9-Bisformyl-5,5-dipropyldipyrromethane (5). In a 250 mL round-bottom flask, 5.00 g (21.7 mmol) of 5,5-dipropyldipyrromethane was dissolved in 100 mL of DMF and cooled to 0 °C. Next, 2.5 equiv of $POCl_3$ (5.0 mL, 53.6 mmol) was added. After stirring for 4 h, the solution was made basic with concentrated aqueous NaOH (the effective solution pH = 11) and heated to reflux and held there for 2 h. Finally, the reaction mixture was quenched with water, extracted with ethyl acetate, and dried over anhydrous Na_2SO_4. Purification via column chromatography on silica gel (eluent: dichloromethane:ethyl acetate, 2:1) gave **5** in 77% isolated yield (4.81 g, 16.80 mmol). ^{1}H NMR (400 MHz, DMSO-d_6): δ 11.63 (bs, 2H, NH), 9.34 (s, 2H, CHO), 6.88 (dd, J = 3.6 Hz, 3.6 Hz, 2H, pyrrolic CH), 6.08 (dd, J = 3.6 Hz, 3.6 Hz, 2H, pyrrolic CH), 2.11 (m, 4H, propyl CH_2), 0.99 (m, 4H, propyl CH_2), 0.84 (t, J = 7.2 Hz 6H, propyl CH_3). ^{13}C NMR (100 MHz, DMSO-d_6): δ 178.75, 146.41, 132.80, 109.22, 43.34, 37.14, 17.04, 14.47. CI-HRMS: M^+ m/z 287.175953 (calcd for $C_{17}H_{23}N_2O_2$ 287.176221). Anal. Calcd for $C_{17}H_{22}N_2O_2$: C, 71.30; H, 7.74; N, 9.78. Found: C, 71.51; H, 7.89; N, 9.70.

Preparation of Dipropyl Schiff Base Macrocycle 4, ($C_{46}H_{52}N_8$). 1,9-Bisformyl-5,5-dipropyldipyrromethane (**5**) (48.6 mg, 1.70 mmol) and *o*-phenylenediamine (184 mg, 1.70 mmol) were dissolved in 75 mL of methanol in a 250 mL round-bottom flask equipped with a magnetic stirrer, reflux condenser, and argon inlet. The solution was warmed to 50 °C, and a few drops of concentrated hydrochloric acid were added to the flask. The faintly yellow colored solution immediately turned a dark red. The solution was then stirred for 3 h at 50 °C and subsequently allowed to cool to ambient temperature. Triethylamine (0.5 mL) was then added, and this produced a yellow flocculent precipitate. The precipitate was collected on a medium porosity glass frit, then redissolved in 20 mL of dichloromethane, and washed with saturated aqueous $NaHCO_3$ (3 × 25 mL). The organic phase was dried over Na_2SO_4, and, after the $NaSO_4$ was filtered off, the solvent was removed in vacuo to give **4** as a yellow-brown glass (295 mg, 0.411 mmol) in 48% yield. ^{1}H NMR (250 MHz, $CDCl_3$): δ 8.06 (s, 4H, imine CH), 7.13 (m, 4H, aromatic CH), 7.01 (m, 4H, aromatic CH), 6.49 (d, J = 3.7 Hz, 4H, pyrrolic CH), 6.08 (d, J = 3.70 Hz, 4H, pyrrolic CH), 2.00 (m, 8H, propyl CH_2), 1.15 (m, 8H, propyl CH_2), 0.90 (t, 12H, propyl CH_3), *NH signals not seen*. ^{13}C NMR (100 MHz, $CDCl_3$): δ 150.38, 144.86, 142.97, 130.38, 125.84, 119.83, 117.13, 108.02, 43.31, 38.75, 17.12, 14.55. CI-HRMS: M^+ m/z 717.437323 (calcd for $C_{46}H_{53}N_8$ 717.439319). Anal. Calcd for $C_{46}H_{52}N_8 \cdot 2H_2O$: C, 73.37; H, 7.50;

(18) Givaja, G.; Blake, A.; Wilson, C.; Schröder, M.; Love, J. B. *Chem. Commun.* **2003**, 2508−2509.
(19) Adams, H.; Bailey, N. A.; Fenton, D. E.; Moss, S.; Debarbarin, C. O. R.; Jones, G. *J. Chem. Soc., Dalton Trans.* **1986**, 693−699.
(20) Adams, H.; Elsegood, M. R. J.; Fenton, D. E.; Heath, S. L.; Ryan, S. J. *J. Chem. Soc., Dalton Trans.* **1999**, 2031−2037.
(21) Sessler, J. L.; Cho, W.-S.; Dudek, S. P.; Hicks, L.; Lynch, V. M.; Huggins, M. T. *J. Porphyrins Phthalocyanines* **2003**, *7*(2), 97−104.
(22) Klose, A.; Solari, E.; Floriani, C.; Chiesi-Villa, A.; Rizzoli, C.; Re, N. *J. Am. Chem. Soc.* **1994**, *116*, 9123−9135.
(23) Machelett, B. *Z. Chem.* **1976**, *16*, 116−117.
(24) Muller, H.; Seidel, W.; Görls, H. *J. Organomet. Chem.* **1993**, *445*, 133−136.

N, 14.88. Found: C, 73.56; H, 7.40; N, 14.95. UV−vis (CH_2Cl_2): λ_{max}, nm (log ϵ) 318 (4.8).

Preparation of μ-Oxo Diiron Complexes 6−10. In a typical reaction, a flame-dried Schlenk flask was charged with 1.0 equiv of the Schiff base macrocycle (**1**−**4**) and allowed to stand overnight under vacuum before being transferred into a drybox, where it was charged with 1.2 to 1.5 equiv of Fe_2Mes_4. After addition of Fe_2Mes_4, the flask was transferred from the drybox to a Schlenk line and cooled to −78 °C. At this point, 25 mL of chilled THF (−78 °C) was cannulated into the flask and the resulting yellow-orange slurry was stirred for 10 min. The cold bath was then removed and the reaction mixture stirred overnight at ambient temperature to give a dark brown solution. The solutions were exposed to air, and the μ-oxo diiron macrocycles **6**−**10** were isolated as dark brown powders in 30−60% yield.

Preparation of 6, [($C_{38}H_{32}N_8$)Fe_2O]. One equivalent of free base **1** (67.0 mg, 0.111 mmol) was reacted with 1.2 equiv of Fe_2Mes_4 (78.0 mg, 0.133 mmol) (in accord with the procedure given above) to give **6** as a dark brown powder. Slow vapor diffusion of *n*-pentane or *n*-hexane into a concentrated CH_2Cl_2 solution of **6** in air gave a brown-black crystalline solid (**6**, 27.9 mg, 42%). CI-HRMS: M^+ *m*/*z* 728.141518 (calcd for $C_{38}H_{32}N_8Fe_2O$ 728.139787). Anal. Calcd for $C_{38}H_{32}N_8Fe_2O\cdot{}^3/_4H_2O\cdot{}^1/_4CH_2Cl_2$: C, 60.20; H, 4.49; N, 14.68. Found: C, 60.53; H, 5.01; N, 14.33. UV−vis (CH_2Cl_2): λ_{max}, nm (log ϵ) 318 (4.7). This compound was also characterized by X-ray diffraction analysis (see below).

Preparation of 7, [($C_{42}H_{40}N_8O_4$)Fe_2O]. One equivalent of free base **2** (32.0 mg, 0.0441 mmol) was reacted with 1.5 equiv of Fe_2Mes_4 (39.0 mg, 0.0663 mmol) (in accord with the procedure given above) to give **7** as a dark brown powder. Slow vapor diffusion of *n*-pentane or *n*-hexane into a concentrated CH_2Cl_2 solution of **7** in air gave a brown-black crystalline solid (**7**, 19.5 mg, 52%). CI-HRMS, M^+ *m*/*z* 848.181720 (calcd for $C_{42}H_{40}N_8Fe_2O_5$ 848.182045). Anal. Calcd for $C_{42}H_{40}Fe_2N_8O_5\cdot{}^3/_4CH_2Cl_2$: C, 56.29; H, 4.59; N, 12.28. Found: C, 56.36; H, 4.42; N, 12.36. UV−vis (CH_2Cl_2): λ_{max}, nm (log ϵ) 311 (4.9). This compound was also characterized by X-ray diffraction analysis (see below).

Preparation of 8, [($C_{46}H_{48}N_8$)Fe_2O]. One equivalent of free base **4** (43.0 mg, 0.0600 mmol) was reacted with 1.5 equiv of Fe_2Mes_4 (53.0 mg, 0.0901 mmol) (in accord with the procedure given above) to give **8** as a dark brown powder. Slow vapor diffusion of hexanes into a concentrated CH_2Cl_2 solution of **8** in air gave a brown-black crystalline solid (24.5 mg, 48%). CI-HRMS: M^+ *m*/*z* 840.264829 (calcd for $C_{46}H_{48}N_8Fe_2O$ 840.264987). Anal. Calcd for $C_{46}H_{48}Fe_2N_8O\cdot{}^1/_3C_6H_{14}$: C, 65.41; H, 6.18; N, 12.71. Found: C, 65.69; H, 6.12; N, 12.59. UV−vis (CH_2Cl_2): λ_{max}, nm (log ϵ) 312 (4.9). This compound was also characterized by X-ray diffraction analysis (see below).

Preparation of 9, [($C_{42}H_{42}N_8O_4$)Fe_2Cl_2O]. One equivalent of **2**·2HCl (57.5 mg, 0.0721 mmol) was reacted with 1.4 equiv of Fe_2Mes_4 (57.9 mg, 0.0984 mmol) (in accord with the procedure given above). Slow vapor diffusion of *n*-pentane into a concentrated THF solution gave **9** as a dark crystalline solid (11.0 mg, 17%). Anal. Calcd for $C_{42}H_{42}Cl_2Fe_2N_8O_5\cdot 2C_5H_{12}$: C, 63.58; H, 7.05; N, 10.59. Found: C, 63.48; H, 6.61; N, 10.20. UV−vis (CH_2Cl_2): λ_{max}, nm (log ϵ) 349 (4.8). This compound was also characterized by X-ray diffraction analysis (see below).

Preparation of 10, [($C_{46}H_{50}N_8$)Fe_2Cl_2O]. One equivalent of **3**·2HCl (69.0 mg, 0.0874 mmol) was reacted with 1.2 equiv of Fe_2Mes_4 (62.0 mg, 0.105 mmol) (in accord with the procedure given above). Slow vapor diffusion of hexanes into a concentrated CH_2Cl_2 solution gave **10** as a brown-black crystalline solid (30.9 mg, 38%). Anal. Calcd for $C_{46}H_{50}Cl_2Fe_2N_8O\cdot 3H_2O$: C, 51.71; H, 4.96; N, 11.49. Found: C, 51.64; H, 5.01; N, 11.50. UV−vis (CH_2Cl_2): λ_{max}, nm (log ϵ) 313 (4.7). This compound was also characterized by X-ray diffraction analysis (see below).

X-ray Crystallography. The data were collected on a Nonius Kappa CCD diffractometer using a graphite monochromator with Mo Kα radiation (λ = 0.71073 Å). The data were collected at 153 K using an Oxford Cryostream low-temperature device. Data reduction was performed using DENZO-SMN.[25] The structure was solved by direct methods using SIR97[26] and refined by full-matrix least-squares on F^2 with anisotropic displacement parameters for the non-H atoms using SHELXL-97.[27] The hydrogen atoms on carbon were calculated in ideal positions with isotropic displacement parameters set to $1.2\times U_{eq}$ of the attached atom ($1.5\times U_{eq}$ for methyl hydrogen atoms).

X-ray Experimental for 6, [($C_{38}H_{32}N_8$)Fe_2O]·0.5CH_2Cl_2. Crystals grew as black plates by vapor diffusion of hexanes into a methylene chloride solution of the complex. A total of 250 frames of data were collected using ω-scans with a scan range of 0.9° and a counting time of 319 s per frame. Details of crystal data, data collection, and structure refinement are listed in Table 1.

The ($C_{38}H_{32}N_8$)Fe_2O lies on a crystallographic mirror plane of symmetry that bisects the complex. The mirror located at $y = {}^1/_4$ bisects the Fe−O−Fe moiety passing through the dimethoxy phenyl rings. A molecule of methylene chloride was found to be disordered around a crystallographic mirror plane of symmetry at $y = {}^1/_4$. It also appeared that the bridging O atom was disordered (see the CIF of the Supporting Information for a full description of the disorder in this crystal).

X-ray Experimental for 7, [($C_{42}H_{40}N_8O_4$)Fe_2O]·4CH_2Cl_2. Crystals grew as very thin, dark brown plates by slow evaporation from dichloromethane and hexanes. A total of 292 frames of data were collected using ω-scans with a scan range of 1° and a counting time of 197 s per frame. Details of crystal data, data collection, and structure refinement are listed in Table 1.

X-ray Experimental for 8, [($C_{46}H_{48}N_8$)Fe_2O]·C_6H_{14}. Crystals grew as thin, black lathes by vapor diffusion of hexanes and *n*-pentane into a methylene chloride solution of the complex. A total of 283 frames of data were collected using ω-scans with a scan range of 1° and a counting time of 313 s per frame. Details of crystal data, data collection, and structure refinement are listed in Table 1.

X-ray Experimental for 9, [($C_{42}H_{42}N_8O_4$)Fe_2Cl_2O]·3C_4H_8O. Crystals grew as black lathes by diffusion of *n*-pentane into a tetrahydrofuran solution of the complex. A total of 400 frames of data were collected using ω-scans with a scan range of 1° and a counting time of 227 s per frame. Details of crystal data, data collection, and structure refinement are listed in Table 1.

The Fe atom positions appeared to be disordered. The disorder amounted to an Fe atom coordinating to different sides of the macrocycle. The disorder did not appear to affect the bridging oxygen atom, O1, or the chloride ions. In addition to the disordered Fe atoms, one molecule of THF and a methyl group of a methoxy moiety were also disordered (see the CIF of the Supporting Information for a full description of the disorder in this crystal).

(25) DENZO-SMN. Otwinowski, Z.; Minor, W. In *Methods in Enzymology, Vol. 276: Macromolecular Crystallography*; Carter, C. W., Jr., Sweet, R. M., Eds.; Academic Press: New York, 1997; Part A, pp 307−326.

(26) SIR97. A program for crystal structure solution. Altomare, A.; Burla, M. C.; Camalli, M.; Cascarano, G. L.; Giacovazzo, C.; Guagliardi, A.; Moliterni, A. G. G.; Polidori, G.; Spagna, R. *J. Appl. Crystallogr.* **1999**, *32*, 115−119.

(27) Sheldrick, G. M. *SHELXL97. Program for the Refinement of Crystal Structures*; University of Göttingen: Göttingen, Germany, 1994.

Table 1. Crystal Data and Structure Refinement Parameters for **6**−**10**

	6·0.5CH_2Cl_2	**7**·4CH_2Cl_2	**8**·C_6H_{14}	**9**·3C_4H_8O	**10**·0.5C_6H_{14}
empirical formula	$C_{39}H_{34}Cl_2Fe_2N_8O$	$C_{46}H_{48}Cl_8Fe_2N_8O_5$	$C_{52}H_{62}Fe_2N_8O$	$C_{54}H_{66}Cl_2Fe_2N_8O_8$	$C_{49}H_{57}Cl_2Fe_2N_8O$
fw	813.34	1188.22	926.80	1137.75	956.63
crystal system	orthorhombic	monoclinic	monoclinic	triclinic	monoclinic
crystal color	black plates	black plates	black lathes	black lathes	black plates
space group	*Pnma*	$P2_1/c$	$P2_1/c$	P_1	$P2_1/c$
a, Å	22.9779(13)	19.3235(11)	23.7941(10)	12.9485(3)	17.8779(6)
b, Å	18.8198(9)	11.4123(6)	8.8588(5)	13.4105(3)	15.3460(7)
c, Å	8.2504(4)	23.7326(15)	23.7874(14	17.2908(5)	18.5817(8)
α, deg	90	90	90	106.450(2)	90
β, deg	90	97.258(2)	113.805(2)	92.570(2)	109.606(3)
γ, deg	90	90	90.000(2)	109.053(2)	90
V, Å^3	3567.8(3)	5191.7(5)	4587.5(4)	2690.43(12)	4802.4(3)
Z	4	4	4	2	4
D (calcd), mg/m^3	1.514	1.520	1.342	1.404	1.323
abs coeff, mm^{-1}	1.008	1.023	0.681	0.700	0.760
F(000)	1672	2432	1960	1192	2004
crystal size	0.27 × 0.20 × 0.04	0.29 × 0.24 × 0.03	0.35 × 0.06 × 0.02	0.20 × 0.19 × 0.15	0.30 × 0.25 × 0.11
θ for data collection	3.04−24.99	2.99−23.75	2.96−24.78	3.13−25.00	2.92−25.00
limiting indices	$-27 \le h \le 27$	$-21 \le h \le 21$	$0 \le h \le 27$	$-15 \le h \le 15$	$-21 \le h \le 21$
	$-22 \le k \le 22$	$-12 \le k \le 12$	$0 \le k \le 10$	$-15 \le k \le 15$	$-18 \le k \le 18$
	$-9 \le l \le 9$	$-26 \le l \le 26$	$-28 \le l \le 25$	$-20 \le l \le 20$	$-22 \le l \le 21$
reflns collected	5899	13705	7559	17341	15560
indep reflns	3233	7506	7559	9442	8382
completeness to θ	99.7%	95.0%	95.9%	99.5%	99.3%
absorption correction	none	none	none	none	None
data/restraints/params	3233/43/264	7506/0/623	7559/0/569	9442/443/665	8382/20/542
GOF on F^2 [a]	1.834	1.227	0.985	1.495	1.994
R,[b] R_w[b]	0.0694, 0.138	0.0733, 0.167	0.0839, 0.150	0.0689, 0.1240	0.107, 0.157

[a] Goodness of fit, S, $= [\sum w(|F_o|^2 - |F_c|^2)^2/(n-p)]^{1/2}$. [b] $R = [\sum(|F_o| - |F_c|)/\sum|F_o|]$ for reflections with $F_o > 4(\sum(F_o))$. $R_w = [\sum w(|F_o|^2 - |F_c|^2)^2/\sum w(|F_o|)^4]^{1/2}$.

X-ray Experimental for 10, [($C_{46}H_{50}N_8$)Fe_2Cl_2O]·0.5C_6H_{14}. Crystals grew as black plates by vapor diffusion of *n*-hexane into a dichloromethane solution of the iron macrocyclic complex. A total of 265 frames of data were collected using *ω*-scans with a scan range of 1° and a counting time of 219 s per frame. Details of crystal data, data collection, and structure refinement are listed in Table 1.

A molecule of what appeared to be *n*-hexane was found to be disordered near 0, *y*, $^1/_4$. A view of the unit cell packing reveals that the solvent molecule resides in a columnar shaped cavity parallel to *b*. The contribution to the scattering by the disordered solvent was removed by use of the utility, SQUEEZE, in PLATON98. The results from SQUEEZE indicated that there was one-half of an *n*-hexane molecule per macrocyclic Fe complex. A methyl carbon on an ethyl group, C42, was also found to be disordered about two principal positions (see CIF of the Supporting Information for a full description of the disorder in this crystal).

Results and Discussion

While exploring the anion binding properties of **1**−**3**, we found that these macrocycles could bind either 1 or 2 equiv of chloride anion per ligand unit. The large core size and ability of these macrocycles to bind multiple anions led us to consider that **1**−**3** could have a role to play as binucleating ligands for metal cations. As mentioned in the Introduction, pyrrolic ligands have a history as metal complexing ligands and, indeed, in limited instances have been used to support the formation of binuclear complexes. In fact, while the present work was in progress, Schröder and Love reported that analogues of macrocycles **1**−**3** could be used to stabilize a bis-Pd(II) complex.[18] Given the more prominent role that iron plays in porphyrin chemistry and its importance in nature, we elected to start our own studies using this element. In the course of these investigations, we became interested in the effect that ligand substitution might have on metal coordination. Macrocycles **1** and **2** each contain methyl substituents at the sp^3 carbon of the dipyrromethane unit while macrocycle **3** is unsubstituted in these positions. To address more precisely the role that steric effects might play, and, in a more general sense, the effect of substitution on metal coordination, we prepared macrocycle **4** (Scheme 1), which contains propyl substituents on the sp^3 carbons.

Synthesis of a Dipropyl Calix[4]pyrrole Schiff Base Macrocycle. The dipropyl calix[4]pyrrole Schiff base, **4**, was prepared by methods similar to those used in the synthesis of ligands **1**−**3**.[21] As shown in Scheme 1, acid-catalyzed condensation of 1,9-bisformyl-5,5-dipropyldipyrromethane (**5**) and *o*-phenylenediamine with HCl in methanol gave the calix[4]pyrrole Schiff base macrocycle **4** as an HCl salt. Triethylamine liberates the free base form of **4** as a yellow flocculent precipitate. The precipitate was collected by filtration, redissolved in CH_2Cl_2, and washed with aqueous $NaHCO_3$ to remove all traces of HCl. Removal of the solvent under vacuum gave spectroscopically pure **4** in 48% yield as a yellow brown glass. Macrocycle **4** was fully characterized by standard techniques (cf. Experimental Section).

Reactions of Calix[4]pyrrole Schiff Base Macrocycles 1−**4 with Iron Salts.** Initial attempts to prepare iron coordinated metal complexes of **1** with simple iron salts, such as $FeCl_2$, $FeCl_3$, and Fe(acetylacetonate)$_3$, in the presence of an organic base did not result in the isolation of any new coordination complexes. The failure to isolate a new metal species under these conditions could be attributed to the strong stability of Fe−Cl and Fe−O bonds in these reagents.

Scheme 1

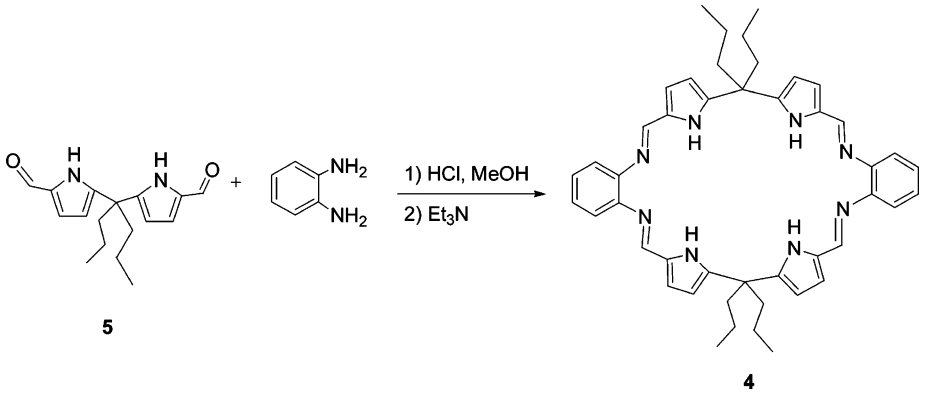

5 **4**

Scheme 2

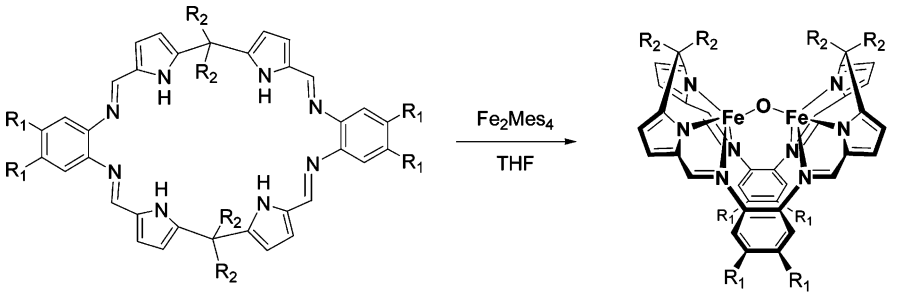

1 R_1 = H, R_2 = CH_3
2 R_1 = OCH_3, R_2 = CH_3
4 R_1 = H, R_2 = $CH_2CH_2CH_3$

6 R_1 = H, R_2 = CH_3
7 R_1 = OCH_3, R_2 = CH_3
8 R_1 = H, R_2 = $CH_2CH_2CH_3$

Scheme 3

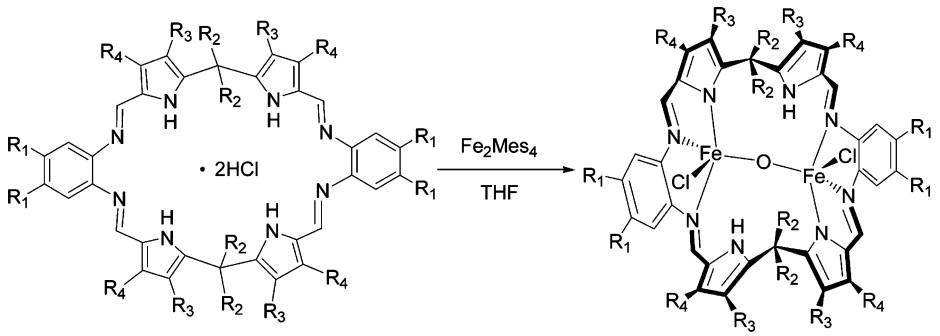

2 (·2HCl) R_1 = OCH_3, R_2= CH_3, R_3= H, R_4= H
3 (·2HCl) R_1 = H, R_2 = H, R_3 = CH_2CH_3, R_4= H

9 R_1 = OCH_3, R_2= CH_3, R_3= H, R_4= H
10 R_1 = H, R_2= H, R_3= CH_2CH_3, R_4= CH_3

Consequently, we sought more labile iron complexes, such as $[Fe(CH_3CN)_6][AlCl_4]_2$.[28] However, even using these kinds of reagents, we still failed to isolate any new metal coordinated macrocycles. Previous work with the protonated forms of macrocycles **1**−**3** revealed their propensity to form anion complexes.[21] Hence, iron reagents, such as $[Fe(CH_3CN)_6][AlCl_4]_2$[28] or $[Fe(CH_3CN)_6][BF_4]_2$,[29] that can generate $H^+[AlCl_4]^-$ and $H^+[BF_4]^-$ in the presence of protic media, were not expected to be good metalating agents for macrocycles **1**−**4** since they might favor the formation of anion complexes, rather than metalated products. However, a reagent such as Fe_2Mes_4[22−24] (Figure 2), having four labile mesityl ligands, is an excellent deprotonating agent and ideal candidate for metalation of **1**−**4**. Indeed, reaction of macrocycles **1**−**4** with Fe_2Mes_4 resulted in new μ-oxo Fe(III) coordinated macrocycles **6**−**10**. In a typical reaction, either the free base form (Scheme 2) or the bis-HCl salt (Scheme 3) of the calix[4]pyrrole Schiff base macrocycle (**1**−**4**) and Fe_2Mes_4 were dissolved in THF at −78 °C, and then allowed to warm to room temperature to give a dark brown solution,

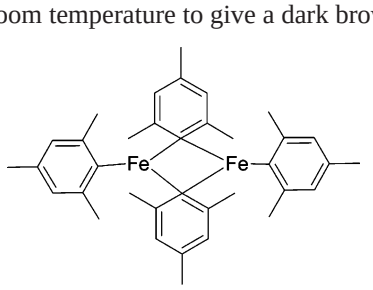

Figure 2. Iron(II) mesitylene, Fe_2Mes_4.

(28) Boudjouk, P.; So, J.-H. *Inorg. Synth.* **1992**, *29*, 111−118.
(29) Heintz, R. A.; Smith, J. A.; Szalay, P. S.; Weisgerber, A.; Dunbar, K. R. *Inorg. Synth.* **2002**, *33*, 75−83.

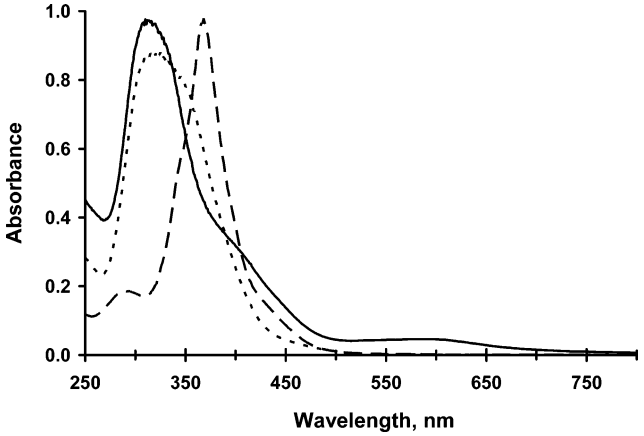

Figure 3. UV−vis spectra of the free base form of **4** (···), the HCl salt of **4** (- - -), and the μ-oxo bis iron complex, **8** (—) in CH_2Cl_2.

which was stirred overnight. The solvent was then removed under vacuum, leaving a brown powder. The bis Fe(III)−μ-oxo complexes **6**−**10** were crystallized by slow diffusion of *n*-pentane or *n*-hexane into concentrated THF (**9**, 15%) or CH_2Cl_2 (**6**−**8**, **10**, 38−52%) solutions of the brown powder. Initial mass spectrometric data (CI or FAB) for the reaction mixture was consistent with the Schiff base macrocycles (**1**−**4**) being converted completely into the corresponding metalated complexes (**6**−**10**). However, yellow-orange powders that formed during crystallization seemed to indicate that some demetalation was occurring, a conclusion that was supported by mass spectrometric analysis. Complexes **6**−**10** were characterized by mass spectrometry, elemental analysis, UV−vis spectroscopy, and X-ray crystallography. All complexes appear to be stable in air as solid dark brown to black powders or crystals. The UV−vis spectra of the free base form and the bis-HCl salt of **4** and μ-oxo bis iron(III) adduct, **8**, are shown in Figure 3. The UV−vis spectra for these three different forms of the dipropyl substituted system, **4**, are all characterized by a single Soret-like absorption band. The spectrum of the bis-HCl salt displays the most red shifted Soret band, while that of the μ-oxo iron complex, **8**, also contains a shoulder around 394 nm and an absorbance centered around 590 nm that is relatively more intense than the other species under study.

Crystallographic Characterization of 6−**10.** Due to the paramagnetic nature of **6**−**10**, the structures of these new complexes were not confirmed by NMR spectroscopy. However, we did obtain suitable crystals of **6**−**10** for single-crystal X-ray diffraction analysis. The resulting structures are shown in Figures 4−8, with selected bond lengths and angles listed in Tables 2 and 3. Examination of these figures reveals that each ligand is bound by two Fe(III) atoms containing a single μ-oxo bridge. However, the nature of this binding differs when the complexes are formed from the free base macrocycles (complexes **6**, **7**, and **8**), rather than from the HCl salts (complexes **9** and **10**). This difference is highlighted in line structures shown in Schemes 1 and 2 (see above).

In the case of complexes **6**−**8** (Figures 4−6), the ligand is significantly folded about the axis containing the two sp^3 carbon atoms. As a result, two phenylene rings of each

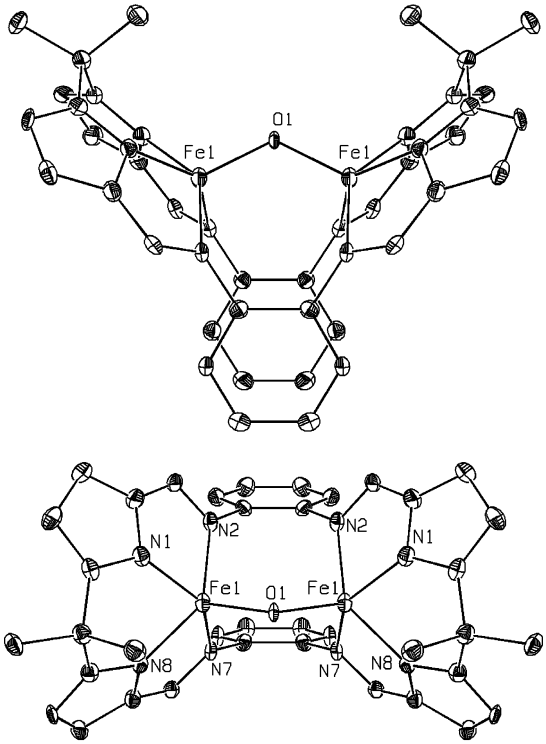

Figure 4. Two views of **6** showing partial atom labeling schemes. Displacement ellipsoids are scaled to the 30% probability level. The hydrogen atoms have been removed for clarity. The complex lies on a crystallographic mirror plane of symmetry at $y = 1/4$. The crystallographic mirror bisects the two phenyl rings and passes through the bridging oxide ion, O1. A half of a molecule of CH_2Cl_2 is contained in the lattice; it is disordered and is not shown.

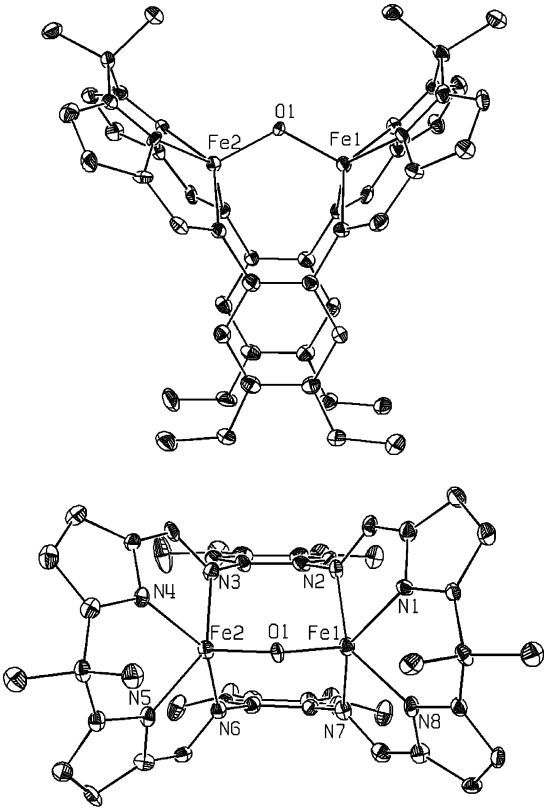

Figure 5. Two views of **7** showing partial atom labeling schemes. Displacement ellipsoids are scaled to the 30% probability level. The hydrogen atoms have been removed for clarity. Four molecules of CH_2Cl_2 which are contained in the lattice are not shown.

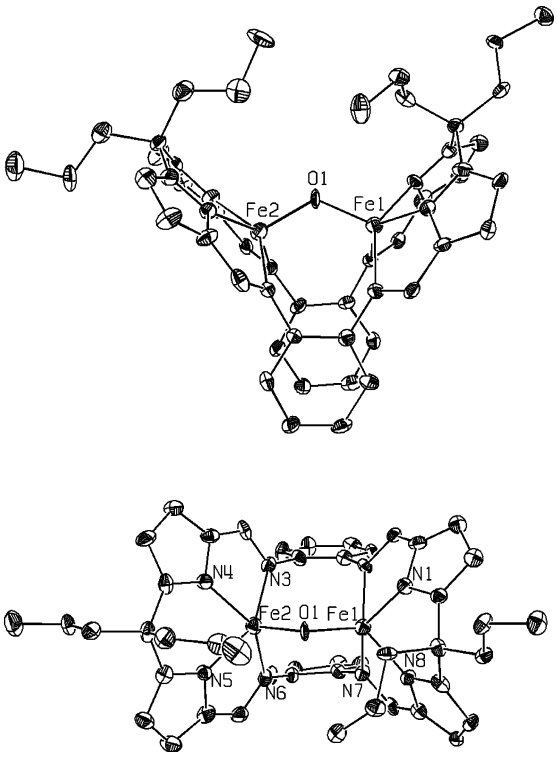

Figure 6. Two views of **8** showing partial atom labeling schemes. Displacement ellipsoids are scaled to the 30% probability level. The hydrogen atoms have been removed for clarity. A molecule of hexane contained in the lattice is not shown.

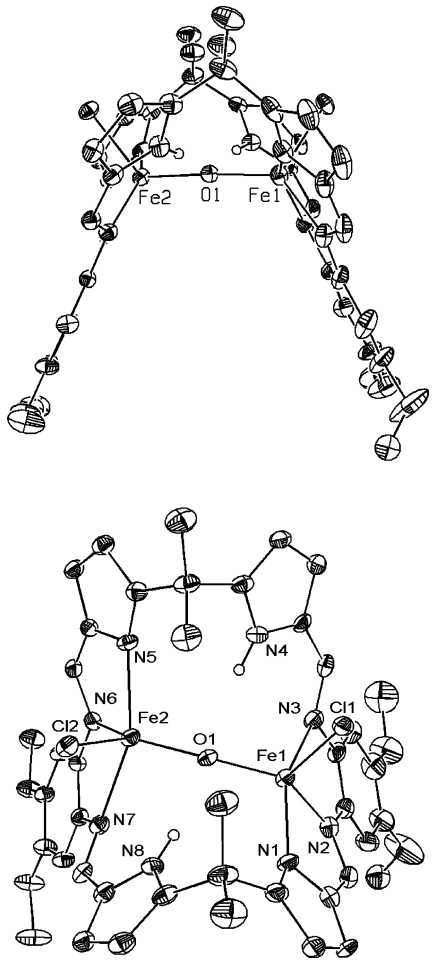

Figure 7. Two views of **9** showing partial atom labeling schemes. Displacement ellipsoids are scaled to the 30% probability level. Most hydrogen atoms have been removed for clarity. Three molecules of THF contained in the lattice are not shown.

macrocycle are stacked relative to one another; this yields a crystallographic mirror plane which bisects the Fe−O−Fe angle in **6** and the approximate mirror planes found in **7** and **8** (the latter two structures have substituents which break the overall symmetry). In this conformation, each Fe atom of the central Fe−O−Fe moiety is coordinated to one dipyrromethane unit (through each pyrrole nitrogen) and to two phenylene diimine units (through one imine nitrogen from each phenylene diimine). In complexes **6**−**8**, each iron center is five coordinate with a geometry that can be described as being a distorted square pyramid. The N−Fe−N angles range between 77.5° and 103.7° for adjacent nitrogen atoms while the N−Fe−O angles range between 101.3° and 115.9°. These angles compare well with those of Fe(III) μ-oxo porphyrin dimers in which the Fe(III) atoms and porphyrin rings are not coplanar (i.e., 86.9° for N−Fe−N and 105.5° for N−Fe−O in $[Fe(TPC)]_2O$[30,31]). The Fe−O−Fe angles for **6**−**8** are between 123.3° and 124.9°. These values lie at the low end of the 114−180° range of angles seen for Fe(III)−O−Fe(III).[31] Presumably, this reflects the short distance between the two Fe metal centers (3.143−3.145 Å) which are bridged by phenylene imine moieties on either side of the Fe−O−Fe bridge. The Fe−O bond distances of 1.772−1.794 Å are typical of μ-oxo diferric compounds (1.73−1.82 Å[32]). The Fe−$N_{pyrrole}$ distances for **6**−**8** (2.009−2.025 Å) are slightly shorter than average Fe−N distances observed for Fe(III) μ-oxo porphyrins {i.e., 2.087 Å for $[Fe(TPP)]_2O$, 2.077 Å for $[Fe(OEP)_2]O$, and 2.065 Å for $[Fe(ODM)_2O]$},[33] while the Fe−N_{imine} bonds for **6**−**8** (2.096−2.176 Å) have slightly longer distances. This underscores the fact that there are two distinct types of Fe(III)−N bonds in **6**−**8** (imine and pyrrole) whereas the bonding in porphyrin complexes is more delocalized.

In contrast to complexes **6**−**8**, the presence of HCl in the ligand starting material vastly alters the binding mode of Fe(III) in these new complexes. Like **6**−**8**, complexes **9** and **10** (Figures 7 and 8) are five coordinate μ-oxo diiron(III) complexes. However, the metal coordination environment is not the same. In complexes **9** and **10,** each Fe atom of an Fe−O−Fe moiety is coordinated to one phenylene diimine unit (through each imine nitrogen), one pyrrole nitrogen from

(30) Abbreviations: $[Fe(TPC)]_2O$, (μ-oxo)bis[(7,8-dihydro-5,10,15,20-tetraphenylporphyrinato)iron(III)]; $[Fe(TPP)]_2O$, (μ-oxo)bis[(5,10,15,20-tetraphenylporphyrinato)iron(III)]; $[Fe(OEP)_2]O$, (μ-oxo)bis[(2,3,7,8,-12,13,17,18-octaethylporphyrinato)iron(III)]; $[Fe(ODM)_2O]$, (μ-oxo)-bis[(2,3,7,8,12,13,17,18-octaethyl-5,15-dimethylporphyrinato)iron-(III)]; $[Fe(Tex)]_2O$, (μ-oxo)bis[(4,5,9,24-tetraethyl-16,17-dimethoxy-10,23-dimethyltexaphyrin)iron(III)] or (μ-oxo)bis[(4,5,9,24-tetraethyl-16,17-dimethoxy-10,23-dimethyl-13,20,25,26,27-pentaazapentacyclo-{20.2.1.1.1.0}heptacosa-3,5,8,10,12,14(19),15,17,20,22,24-undecaene)-iron(III)].

(31) Strauss, S. H.; Pawlik, M. J.; Skowyra, J.; Kennedy, J. R.; Anderson, O. P.; Spartalian, K.; Dye, J. L. *Inorg. Chem.* **1987**, *26*, 724−730.

(32) Kurtz, D. M. *Chem. Rev.* **1990**, *90*, 585−606.

(33) Scheidt, W. R. In *The Porphyrin Handbook*; Kadish, K. M., Smith, K. M., Guilard, R., Eds.; Academic Press: San Diego, 2000; Vol. 3, pp 49−112.

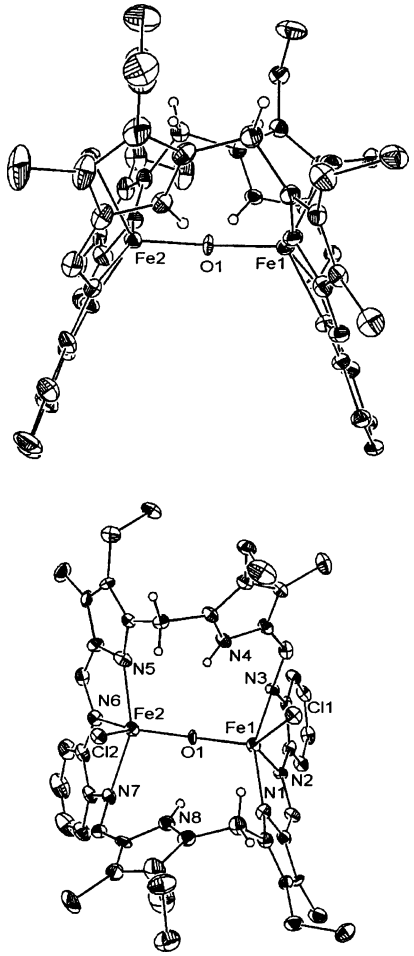

Figure 8. Two views of **10** showing partial atom labeling schemes. Displacement ellipsoids are scaled to the 30% probability level. Most hydrogen atoms have been removed for clarity. One half of a molecule of hexane contained in the lattice is disordered and is not shown.

a dipyrromethane unit, and one Cl atom. In this conformation, the geometry for each iron atom in **9** and **10** can be described as distorted trigonal bipyramidal with N2, Cl1, and O1 as equatorial ligands for Fe1, and N6, Cl2, and O1 as equatorial ligands for Fe2. The angles between these equatorial ligands and iron (114.8−129.4°) and between the corresponding axial ligands and iron (149.5−152.8°) are slightly distorted from trigonal bipyramidal. Unlike complexes **6**−**8**, which are characterized by bent Fe−O−Fe angles (see above), **9** and **10** contain nearly linear Fe−O−Fe angles (177.4° and 176.03°, respectively). These differences are also reflected in the longer Fe···Fe contacts (3.639 and 3.651 Å, respectively), longer Fe−O distances (1.819−1.833 Å), and a larger non-oxo bridging unit, namely, dipyrromethane (**9** and **10**) rather than phenylene diimine (**6**−**8**). The $Fe-N_{pyrrole}$ distances in **9** and **10** (2.090−2.194 Å) are longer than those for **6**, **7**, and **8** (2.009−2.025 Å). The $Fe-N_{imine}$ distances for the imines linkages next to a coordinated pyrrole in **9** and **10** (1.999−2.055 Å) are shorter than those in **6**−**8** (2.096−2.176 Å). The $Fe-N_{imine}$ distances for the imines next to an uncoordinated pyrrole in **9** and **10** (2.218−2.345 Å) are much longer than the $Fe-N_{imine}$ distances in **6**−**8** (2.096−2.176 Å) and longer than those reported for μ-oxo

Table 2. Selected Bond Lengths (Å) and Angles (deg) for **6**−**8**

	6·0.5CH_2Cl_2	**7**·4CH_2Cl_2	**8**·C_6H_{14}
Fe1−O1	1.780(2)	1.777(4)	1.772(5)
Fe2 −O1	*a*	1.794(4)	1.772(5)
Fe1−N1	2.024(5)	2.015(6)	2.017(7)
Fe1−N2	2.135(5)	2.126(6)	2.096(6)
Fe1−N7	2.176(4)	2.134(6)	2.149(7)
Fe1−N8	2.018(4)	2.021(6)	2.004(7)
Fe2−N3	*a*	2.124(6)	2.143(7)
Fe2−N4	*a*	2.014(6)	2.010(7)
Fe2−N5	*a*	2.025(6)	2.009(7)
Fe2−N6	*a*	2.118(6)	2.122(7)
Fe1···Fe2	3.145(2)	3.143(4)	3.143(5)
Fe2−O1−Fe1	124.1(3)	123.3(3)	124.9(3)
N1−Fe1−N2	77.60(17)	77.6(2)	78.4(3)
N1−Fe1−N7	142.54(17)	142.3(2)	144.0(3)
N1−Fe1−N8	81.00(17)	81.3(2)	81.9(3)
N2−Fe1−N7	99.12(16)	100.4(2)	97.4(3)
N2−Fe1−N8	140.74(16)	141.4(2)	137.5(3)
N7−Fe1−N8	78.82(17)	77.8(3)	77.5(3)
N3−Fe2−N4	*a*	78.3(3)	78.9(3)
N3−Fe2−N5	*a*	141.8(2)	145.9(3)
N3−Fe2−N6	*a*	98.6(2)	103.7(3)
N4−Fe2−N5	*a*	81.6(3)	80.5(3)
N4−Fe2−N6	*a*	142.3(2)	143.8(3)
N5−Fe2−N6	*a*	78.5(2)	78.3(3)
N1−Fe1−O1	111.82(19)	110.5(2)	111.1(3)
N2−Fe1−O1	103.64(19)	103.9(2)	106.3(3)
N7−Fe1−O1	105.25(18)	106.5(2)	104.4(3)
N8−Fe1−O1	114.82(19)	113.6(2)	115.9(3)
N3−Fe2−O1	*a*	104.4(2)	101.7(3)
N4−Fe2−O1	*a*	114.1(2)	113.6(3)
N5−Fe2−O1	*a*	113.5(2)	111.4(3)
N6−Fe2−O1	*a*	103.2(2)	101.3(3)

[a] Complex **6** lies on a crystallographic mirror plane of symmetry that bisects the complex. The mirror located at $y = 1/4$ bisects the Fe−O−Fe moiety passing through phenyl rings.

Table 3. Selected Bond Lengths (Å) and Angles (deg) for **9**−**10**

	9·3C_4H_8O	**10**·0.5C_6H_{14}
Fe1−O1	1.820(3)	1.821(4)
Fe2 −O1	1.834(3)	1.819(4)
Fe1−Cl1	2.2698(14)	2.2656(18)
Fe2−Cl2	2.2622(12)	2.2685(17)
Fe1−N1	2.193(4)	2.090(5)
Fe1−N2	1.998(4)	2.053(5)
Fe1−N3	2.346(4)	2.218(5)
Fe1···N4	3.318	3.259
Fe2−N5	2.175(3)	2.092(6)
Fe2−N6	2.006(4)	2.055(5)
Fe2−N7	2.309(4)	2.221(5)
Fe2···N8	3.335	3.257
Fe1···Fe2	3.651	3.639(4)
Fe2−O1−Fe1	176.03(17)	177.4(2)
N1−Fe1−N2	80.32(16)	78.0(2)
N1−Fe1−N3	152.77(14)	149.5(2)
N2−Fe1−N3	73.02(15)	74.52(19)
N1−Fe1−O1	104.34(14)	104.29(19)
N2−Fe1−O1	129.39(15)	119.89(19)
N3−Fe1−O1	96.89(12)	100.78(19)
N1−Fe1−Cl1	93.42(11)	92.26(14)
N2−Fe1−Cl1	115.18(12)	125.31(15)
N3−Fe1−Cl1	92.95(11)	92.85(13)
Cl1−Fe1−O1	114.77(10)	114.79(14)
N5−Fe2−N6	79.29(15)	76.8(2)
N5−Fe2−N7	151.62(13)	149.5(2)
N6−Fe2−N7	73.88(14)	75.2(2)
N5−Fe2−O1	105.82(14)	105.0(2)
N6−Fe2−O1	128.35(13)	122.5(2)
N7−Fe2−O1	98.07(12)	100.18(19)
N5−Fe2−Cl2	92.59(9)	91.59(15)
N6−Fe2−Cl2	115.79(11)	122.25(16)
N7−Fe2−Cl2	90.85(10)	93.06(13)
Cl2−Fe2−O1	115.25(9)	115.19(13)

porphyrins (see above). However, they are not as long as those reported for $[Fe(Tex)]_2O$ (2.051 and 2.494 Å).[34]

Conclusions

A series of unique μ-oxo Fe(III) complexes of Schiff base macrocycles **1**−**4** has been prepared. These new μ-oxo Fe(III) complexes, **6**−**10**, represent the first examples of a class of compounds in which a single pyrrolic binucleating macrocycle has been shown to coordinate a bis-Fe, M−O−M moiety within its core. We have further shown that the nature of the μ-oxo Fe(III) complex is affected by the protonation state of macrocycle.[35] In particular, the structures of the μ-oxo Fe(III) complexes that are formed from the free base macrocycles are very different from those formed from the corresponding HCl salts even when the same starting Fe(II) mesitylene reagent is used in both cases. On the other hand, the specifics of the substitution pattern on the macrocycle seems to have relatively little affect. This is underscored by the fact that the free base macrocycles **1**, **2**, and **4**, bearing different substituents, all give rise to complexes (**6**−**8**) that have bent Fe−O−Fe substructures. By contrast, the use of the bis-HCl salts of **2** and **3** produce complexes (**9** and **10**) that are characterized by essentially linear Fe−O−Fe bridges. The differences seen in these two sets of complexes are expected to affect the overall stability and reactivity of these compounds. Studies to investigate this reactivity are now underway. We are also exploring whether macrocycles **1**−**4**, or their protonated salts, may be used to stabilize complexes containing other transition metal centers. To date we have obtained evidence that leads us to suggest that **1** forms mixed valence μ-oxo Mn(II)/Mn(IV) clusters.[36]

Acknowledgment. This work was supported by the National Institutes of Health (Grant No. CA 68682 to J.L.S. and Grant No. GM20834-02 to J.M.V.).

Supporting Information Available: Complete X-ray structural data and UV−vis spectra for **6**−**10**. This material is available free of charge via the Internet at http://pubs.acs.org.

IC0352001

(34) Hannah, S.; Lynch, V. M.; Guldi, D. M.; Gerasimchuk, N. N.; MacDonald, C. L. B.; Magda, D.; Sessler, J. L. *J. Am. Chem. Soc.* **2002**, *124*, 8416−8427.

(35) The protonation state of the starting ligand appears to be the primary factor that determines the coordination mode of the Fe−O−Fe moiety. However, the presence of a coordinating anion (Cl^-) in the metal free macrocycle could also influence the nature of the Fe−O−Fe moiety.

(36) An X-ray crystal structure shows two units of **1** bound to a disordered cage of 6−8 Mn atoms and 8 oxygen atoms.